GSA DATA REPOSITORY

Seawater chemistry driven by supercontinent assembly, break-up and dispersal

R. D. Müller, A. Dutkiewicz, M. Seton, and C. Gaina

Methodology

For computing the oceanic hydrothermal fluid flux through time we use Jurassic-Cenozoic reconstructions of the oceanic age-area distribution from Seton et al. (2012). We reconstruct absolute plate motions by merging a moving hotspot (O'Neill et al., 2005) (after 100 Ma) and true polar wander–corrected (before 100 Ma) paleomagnetic reference frame (Steinberger and Torsvik, 2008). The uncertainties of reconstructing mid-ocean ridges and flanks in the Jurassic (~200-145 Ma) are substantial, and arguably hard to quantify given that we depend on information preserved in present-day ocean crust. However, in the following we argue that even though the details of those mid-ocean ridge geometries are unknown, we can make reasonable, and conservative, estimates applying Occam's razor paired with the rules of plate tectonics as a guide to available geophysical and geological data constraining mid-ocean ridge geometries through time.

Preserved magnetic lineations in the Pacific Ocean provide unequivocal evidence that a vast mid-ocean ridge system existed in the Pacific Ocean in the mid/late Cretaceous, significantly longer than today's ridge system, and much of which is now subducted – this was first recognised by Larson and Chase (Larson and Chase, 1972). Subsequent detailed mapping and compilation of magnetic M-sequence anomalies in the northwestern Pacific Ocean (Nakanishi et al., 1992) revealed the complete Mesozoic magnetic anomaly lineation pattern in this area. Nakanishi et al. (1992) wrote that "Reconstruction of the Late Jurassic lineations (e.g., in the East Mariana, Nauru and Central Pacific basins) reveals an exact shape of the Pacific plate in that period" – implying that the mid-ocean ridge system bounding the Pacific plate can be reconstructed in detail all the way back to the Jurassic. Their work also revealed the origin of the Pacific plate as a triangularly shaped microplate at a triple junction in the Panthalassa Ocean basin, the predecessor of the Pacific Ocean. This work forms the basis of our Pacific Ocean reconstructions.

The longest now vanished mid-ocean ridge that once formed part of this ridge system is the Izanagi-Pacific ridge. Nakanishi et al. (1992) emphasized that the complete pattern of magnetic lineations preserved on the Pacific Plate reveals the configuration of the Pacific Izanagi-Farallon triple junction, as the magnetic bight between the Japanese and Hawaiian lineation sets is clearly identified. There are uncertainties associated with reconstructing the exact history of ridge subduction, asymmetries of spreading where we only have information on one plate preserved, and several other aspects of the exact mid-ocean ridge configuration in the Pacific Ocean in the Mesozoic. However, it is the indisputable history of the birth of the Pacific Plate as a triangular microplate and its subsequent growth to an enormous plate surrounded by a mid-ocean ridge system large parts of which were later subducted (see also reconstructions by Engebretson et al. (1985)) that caused the Cretaceous ocean basins to be at least 25 Myr younger on average compared with today's ocean basins (Müller et al., 2008b), associated with equivalent more voluminous hydrothermal fluid flux. We assume that the triple junction between the Izanagi, Farallon and Phoenix plates that is known to have existed in the Late Jurassic based on magnetic lineations preserved in the west Pacific Ocean (Nakanishi et al., 1992), existed in similar form since the early Jurassic at 200 Ma and we assume constant spreading rates between the Izanagi, Phoenix and Farallon plates between 200 and 170 Ma, corresponding to the time interval for which no magnetic lineations are preserved.

The revised reconstructions from Seton et al. (2012) we use here include recently proposed models for the opening of ocean basins between fragments of the Ontong Java-Manihiki-Hikurangi large igneous provinces (Taylor, 2006; Viso et al., 2005) (Fig. DR1). Previous reconstructions of the Cretaceous Pacific Ocean (Müller et al., 2008b) basin did not include these mid-ocean ridges, and would have underestimated hydrothermal flux from ridge crests and flanks during the Cenozoic Normal Superchron (~120-83 Ma). In the Tethys, we follow the model by Stampfli and Borel (2002) and Golonka (2007), in which the Paleo-Tethys ocean is closed in the Late Triassic/Early Jurassic, associated with the stepwise collision of a series of Gondwanaland ribbon continents with Eurasia. By using combined evidence from preserved magnetic lineations, and geological data from accreted terranes such as “Argo Land” and the rules of plate tectonics (Cox and Hart, 1986) it is possible to constrain the overall geometries of Tethys mid-ocean ridges quite well, as demonstrated by Heine et al. (2004). The closure of the Mongol-Okhotsk Ocean between 200 and 150 Ma is modelled after van der Voo et al. (1999). In our model the breakup of the supercontinent Pangaea occurs in the central North Atlantic around 200 Ma (Labails et al., 2010) followed by the formation of the Pacific plate about 190 Ma (Seton et al., 2012). In summary, there is evidence for a number of old mid-ocean ridge flanks in the proto-Pacific and the Tethys oceans gradually being destroyed between 200 and 150 Ma, while new mid-ocean ridge systems were initiated in a stepwise fashion between the Late Jurassic and Early Cretaceous, which did not exist before, leading to a substantial younging of the ocean basins from the Jurassic to the Cretaceous period.

Isochrons expressed in magnetic lineations and preserved on present-day ocean floor, together with the rules of plate tectonics, allow us to check a given plate reconstruction solution for self-consistency. In addition, other pieces of geological and paleomagnetic evidence from accreted terranes, as well as global sea level curves, can be used to create a set of ocean floor reconstructions that best satisfies all available data, an approach recently summarized nicely by Ruban et al. (2010). This approach results in an overall growth of ridge flanks between 200 and 100 Ma, followed by a decline in ridge flank area due to progressive flank subduction (Fig. DR1).

Based on our global grid of the age-area extent of ocean floor through time (Fig. DR1) we compute grids of paleo-oceanic heat flow (Fig. DR2), residual heat flow, basement temperature (Fig. DR3), and hydrothermal fluid flux (Figs DR4, DR5, DR6) in 5 Myr intervals by adapting the methodology from Johnson and Pruis (2003). They used a compilation of crustal porosities, heat flow and sediment thickness to compute hydrothermal reservoir temperatures and mean hydrothermal flux into the deep ocean as a function of crustal age (their equation 3). There is observational evidence that other factors such as large-scale ridge reorganisations can modulate hydrothermal fluid flux (Lyle et al., 1985), but these relationships have not yet been quantified and are therefore not included in our analysis. We approximate hydrothermal fluid flux as a function of residual heat flow (the difference between heatflow predicted from a conducting thermal boundary layer model and observed heatflow) and basement temperature (Johnson and Pruis, 2003).

Deep water temperatures in the early Cenozoic and Cretaceous in a largely ice-free world are known to have been higher than present-day deep sea temperatures (D'Hondt and Arthur, 2002; Huber et al., 2002; Lear et al., 2000; Tripati and Elderfield, 2005). However, it is impossible for us to consider these variations quantitatively in terms of correcting our basement temperature grids for this effect, for a number of reasons. At first order, basement temperature is dependent on the cooling of the lithospheric thermal boundary layer and on sediment thickness as a function of crustal age, whereas bottom water temperature only has a small effect on basement temperature on young portions of mid-ocean ridge flanks without sediment cover. Published deep-water temperature estimates are confined largely to the last 100 million years, only covering half of the time period subject to our analysis. In addition, where they are based on Mg/Ca ratios of benthic foraminifers (see Lear et al. (2000)) one of the underlying methodological assumptions is that the Mg/Ca ratio of seawater through time is known. Even though it is well established that this ratio was higher in the Cretaceous and Early Cenozoic than today, the magnitude of this change is subject to considerable debate. An independent study of the magnitude of these fluctuations would be hampered by including deep-sea temperature fluctuations that are based on assuming a particular model for Mg/Ca ratio changes through time.

Analyses of residual oceanic heatflow (Stein and Stein, 1994) suggest that the crustal hydrothermal reservoir becomes isolated from seawater near 65 Myr-old crust. We therefore mask all crust older than 65 Myr for our calculations. Paleo-oceanic crustal age uncertainty grids are computed using an established methodology (Müller et al., 2008a; Müller et al., 2008b) and propagated into errors of paleo-oceanic crustal area for 0-1 and 1-65 Myr-old crust, heat flow, residual heat flow, and fluid flux. Magnetic anomaly identifications were reconstructed to their conjugate ridge flanks for constraining palaeo-mid-ocean ridge locations using the rotations listed by Seton et al. (2012). In areas where one flank of a mid-ocean ridge system has been subducted, we assume spreading symmetry to reconstruct the subducted flank. This is a reasonable assumption given that globally the maximum cumulative spreading asymmetry has been found to be only 10% (Müller et al., 1998).

Recent work (Spinelli and Harris, 2011) suggests that on axis hydrothermal cooling results in a higher percentage of heat extraction than previously calculated. The reason is that some time is needed to increase crustal temperatures via conductive reheating at the ridge flanks once deeper fluid circulation ceases and the crust moves away from the ridge crest. This process results in an increase of 10% in hydrothermal heat extraction for crust younger than 1 Ma, but does not affect the analysis presented in this paper as our arguments are strongly focused on the evolution of ridge flanks older than just a few million years.

Three computed hydrothermal fluid flux ridge flank profiles at 0, 100, and 200 Ma (Fig. DR7) illustrate the similarity between the crustal age-dependence of the hydrothermal fluid flux in the Jurassic and at present, both representing aragonite seas.

The data for all digital grids that this work is based on will be made available on ftp://ftp.earthbyte.org.

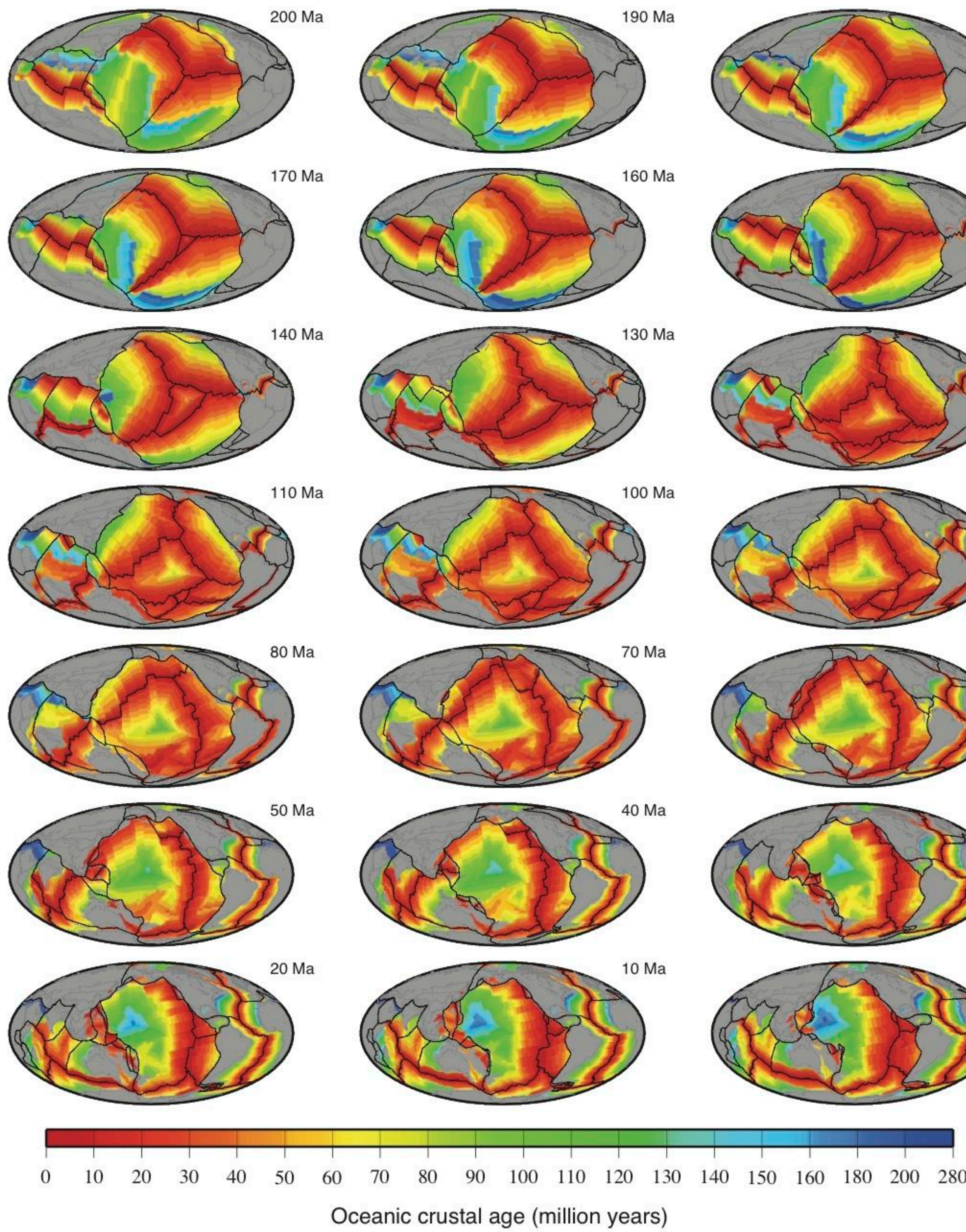

Figure DR1. Oceanic age-area distribution since 200 Myr ago derived from Seton et al.'s (2012) reconstructions and seafloor isochrons.

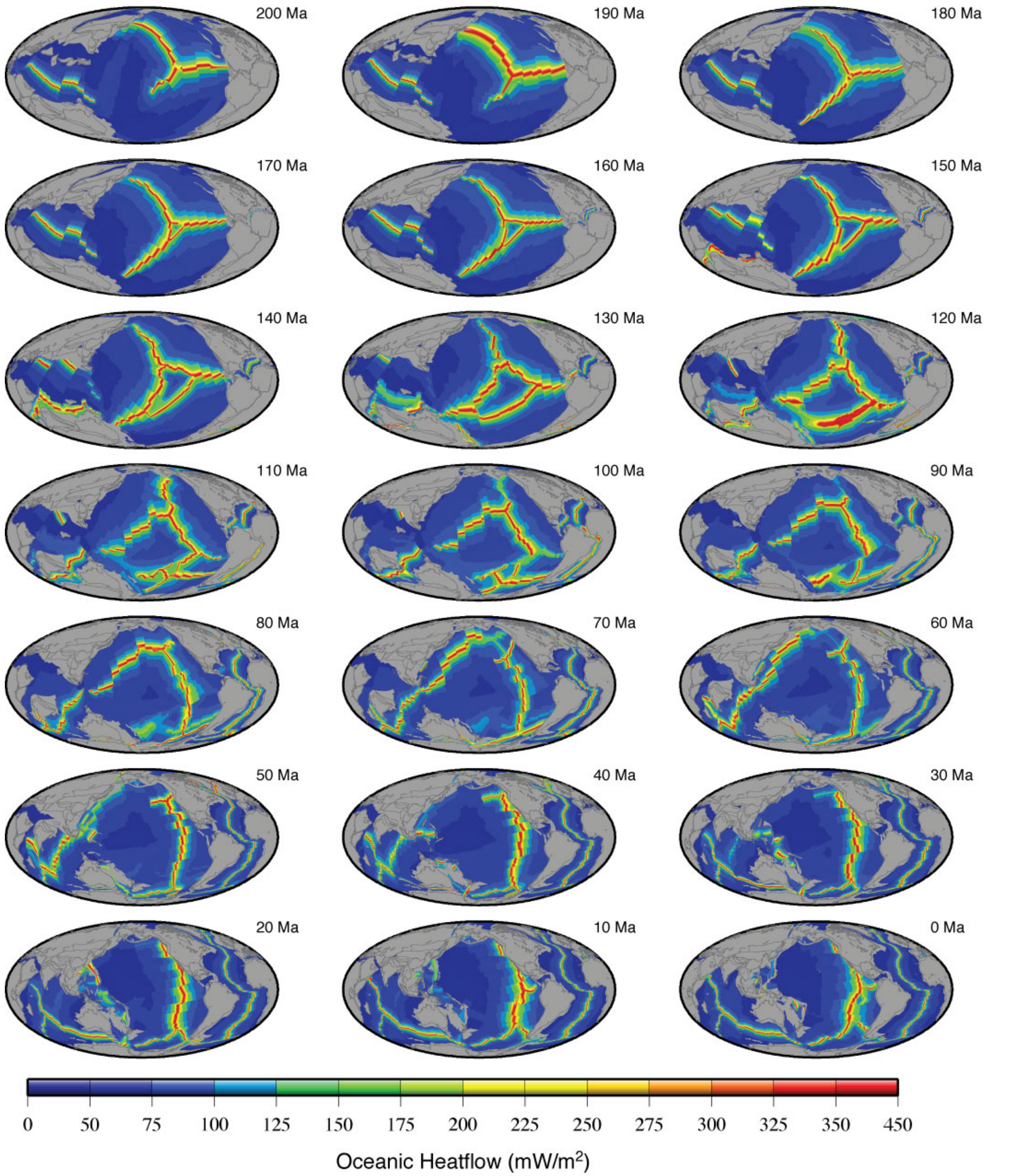

Figure DR2. Oceanic heat flow-area distribution since 200 Myr ago calculated using an established age-heat flow relationship (Stein and Stein, 1992) applied to the oceanic crustal age-area distributions shown in Figure DR1.

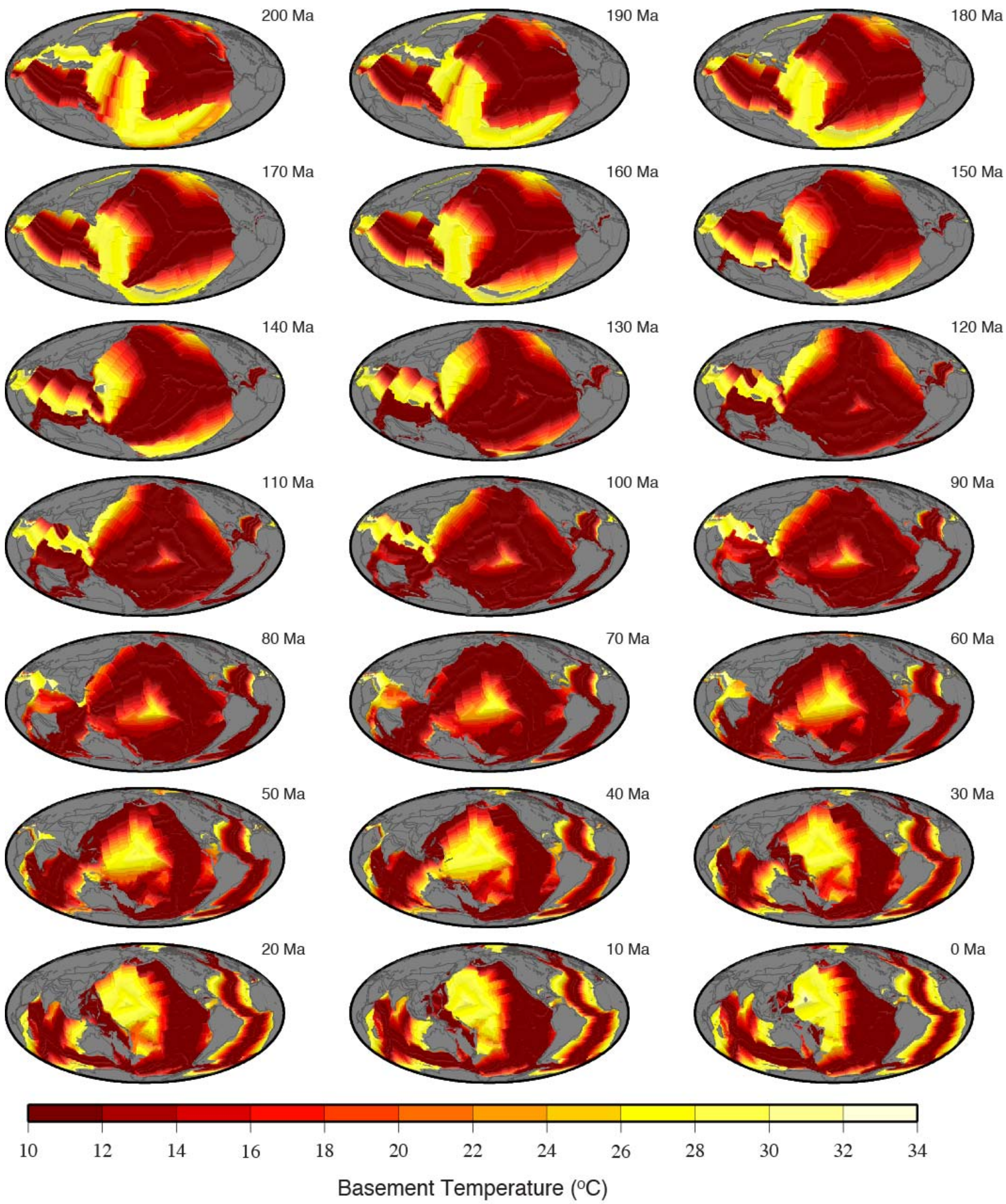

Figure DR3. Oceanic basement temperature since 200 Myr ago based on the grids shown in Figure DR1 and Johnson and Pruis' (2003) age-basement temperature relationship.

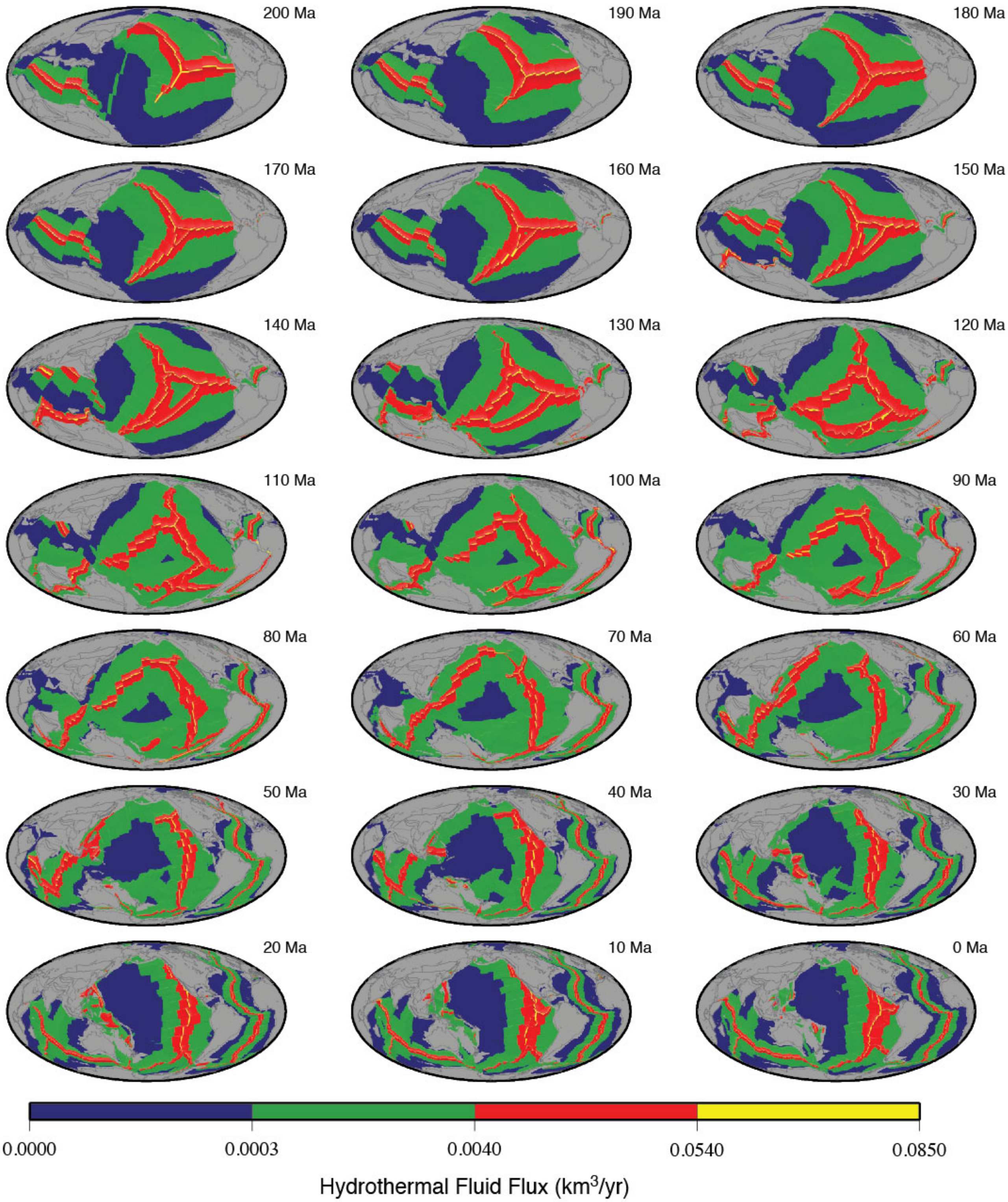

Figure DR4. Oceanic hydrothermal fluid flux since 200 Myr ago based on residual heat flux estimation derived from grids shown in Suppl. Fig. 2, in units of km^3/yr per unit area sized 0.1x0.1 degrees, taking into account the average size (in km^2) of this area given the global latitudinal distribution of grid cells contributing to fluid flux. Fluid flow in crust aged 0-1 Myr shown in yellow, in crust aged 1-20 Myr in red and in crust aged 20-65 Myr old in green.

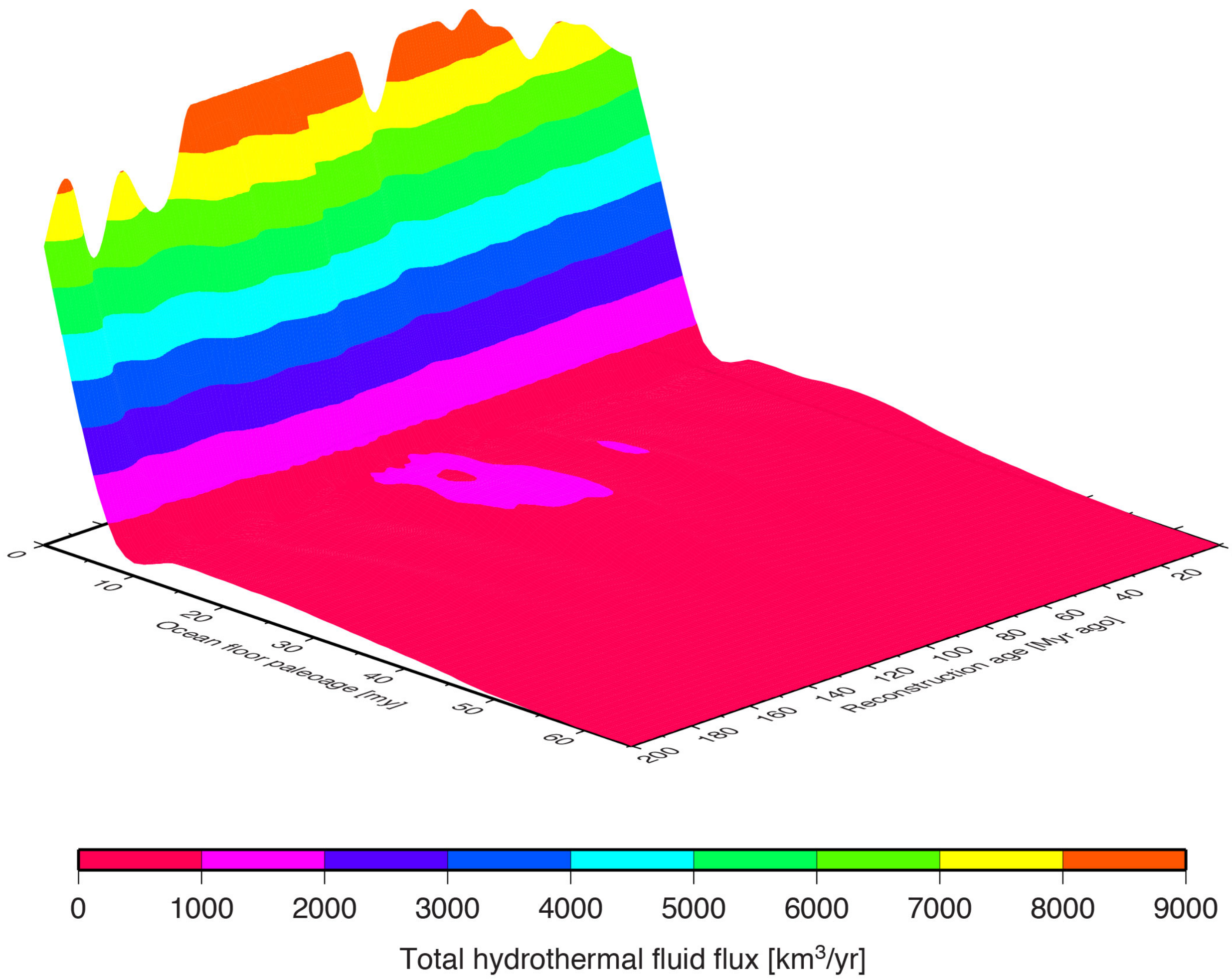

Figure DR5. Dependence of total global hydrothermal flux on ocean floor paleo-age (0-65 Myr) and reconstruction time (0-200 Ma).

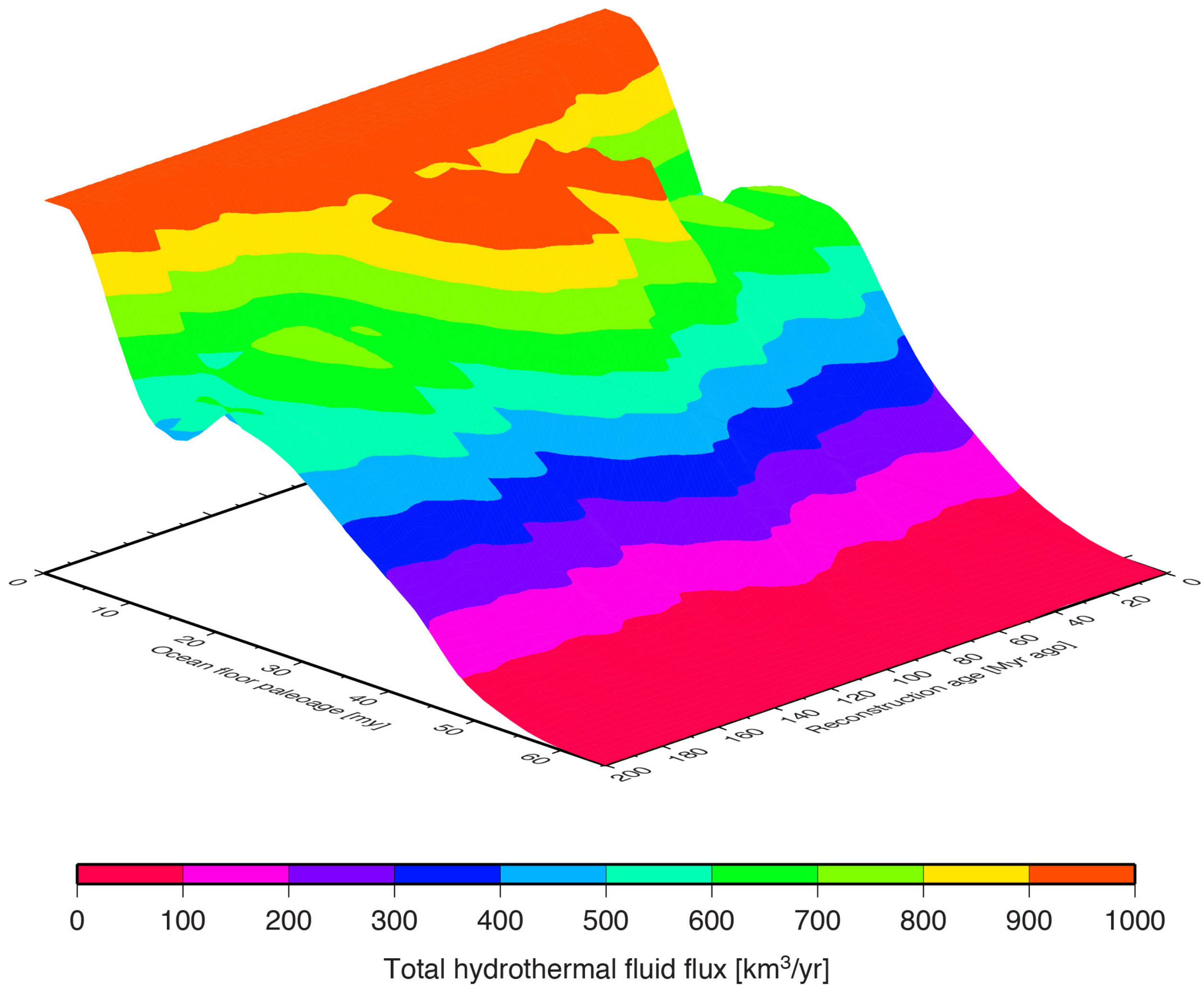

Figure DR6. Dependence of total global hydrothermal flux on ocean floor paleo-age (0-65 Myr) and reconstruction time (0-200 Ma) but with hydrothermal flux on young ocean floor clipped at 1000 km^3/yr to visually enhance volume flux variations on ridge flanks. Note that for most of the Cretaceous period (~ 145 to 65 Ma) volume flux on ridge flanks aged between 0 and 40 Myr is substantially enhanced, illustrating the contribution ridge flanks make to the fluid and chemical fluxes through time.

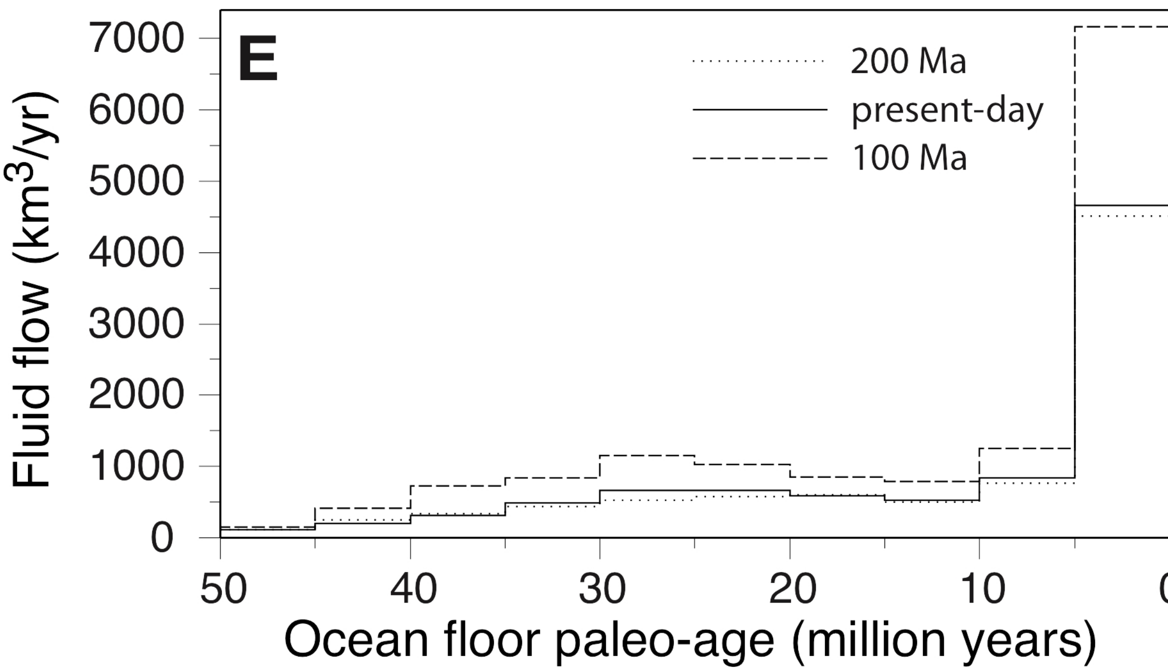

Figure DR7: Computed global fluid flux as a function of ocean floor age in 5 Myr bins from 0-50 Myr-old crust for the present, 100 Ma and 200 Ma. Note the similarity of fluid flow profiles at aragonite sea times 0 and 200 Ma, and the elevated fluid flux from 0-45 Myr old crust at 100 Ma, when calcite seas prevailed.

References

Cox, A., and Hart, B.R., 1986, Plate Tectonics : How It Works, Blackwell Science Inc., 400 p.

D'Hondt, S., and Arthur, M.A., 2002, Deep water in the Late Maastrichtian Ocean: Paleoceanography, v. 17, p. 10.1029/1999PA000486.

Engebretson, D.C., Cox, A., and Gordon, R.G., 1985, Relative motions between oceanic and continental plates in the Pacific Basin: Special Paper, v. 206, p. 1-59.

Golonka, J., 2007, Late Triassic and Early Jurassic palaeogeography of the world: Palaeogeography, Palaeoclimatology, Palaeoecology, v. 244, p. 297-307.

Heine, C., Müller, R.D., and Gaina, C., 2004, Reconstructing the Lost Eastern Tethys Ocean Basin: Convergence history of the SE Asian margin and marine gateways, *in* Clift, P.D., Hayes, D.E., Kuhnt, W., and Wang, P., eds., Continent-Ocean Interactions within East Asian Marginal Seas, AGU Geophysical Monograph, Volume 149: Washington, American Geophysical Union, p. 37-54.

Huber, B.T., Norris, R.D., and MacLeod, K.G., 2002, Deep-sea paleotemperature record of extreme warmth during the Cretaceous: Geology, v. 30, p. 123.

Johnson, H.P., and Pruis, M.J., 2003, Fluxes of fluid and heat from the oceanic crustal reservoir: Earth and Planetary Science Letters, v. 216, p. 565-574.

Labails, C., Olivet, J.L., Aslanian, D., and Roest, W.R., 2010, An alternative early opening scenario for the Central Atlantic Ocean: Earth Planet. Sci. Lett., v. 297, p. 355-368.

Larson, R.L., and Chase, C.G., 1972, Late Mesozoic Evolution of the Western Pacific: Geological Society of America Bulletin, v. 83, p. 3627-3644.
Lear, C., Elderfield, H., and Wilson, P., 2000, Cenozoic deep-sea temperatures and global ice volumes from Mg/Ca in benthic foraminiferal calcite: Science, v. 287, p. 269.
Lyle, M.W., Owen, R.M., and Leinen, M., 1985, History of hydrothermal sedimentation at the East Pacific Rise, *in* Leinen, M., and Rea, D.K., eds., Initial Reports DSDP 92: Washington.
Müller, R.D., Roest, W.R., and Royer, J.-Y., 1998, Asymmetic seafloor spreading expresses ridge-plume interactions: Nature, v. 396, p. 455-459.
Müller, R.D., Sdrolias, M., Gaina, C., and Roest, W.R., 2008a, Age, spreading rates and spreading asymmetry of the world's ocean crust: Geochemistry, Geophysics, Geosystems, v. 9, p. Q04006, doi:10.1029/2007GC001743
Müller, R.D., Sdrolias, M., Gaina, C., Steinberger, B., and Heine, C., 2008b, Long-term sea level fluctuations driven by ocean basin dynamics: Science, v. 319, p. 1357-1362.
Nakanishi, M., Tamaki, K., and Kobayashi, K., 1992, A new Mesozoic isochron chart of the northwestern Pacific Ocean: paleomagnetic and tectonic implications: Geophysical Research Letters, v. 19, p. 693-6.
O'Neill, C.J., Müller, R.D., and Steinberger, B., 2005, On the Uncertainties in Hotspot Reconstructions, and the Significance of Moving Hotspot Reference Frames: Geochemistry, Geophysics, Geosystems, v. 6, p. doi:10.1029/2004GC000784.
Ruban, D.A., Conrad, C.P., and van Loon, A.J.T., 2010, The challenge of reconstructing the Phanerozoic sea level and the Pacific Basin tectonics: Geologos, v. 16, p. 235-243.
Seton, M., R.D., M., Zahirovic, S., Gaina, C., Torsvik, T., G., S., Talsma, A., Gurnis, M., Turner, M., and Maus, S., 2012, Global continental and ocean basin reconstructions since 200 Ma: Earth Science Reviews, v. 113, p. 212-270.
Spinelli, G., and Harris, R., 2011, Effects of the legacy of axial cooling on partitioning of hydrothermal heat extraction from oceanic lithosphere: Journal of Geophysical Research, B, Solid Earth and Planets, v. 116, p. 1-10.
Stampfli, G.M., and Borel, G.D., 2002, A plate tectonic model for the Paleozoic and Mesozoic constrained by dynamic plate boundaries and restored synthetic oceanic isochrons: Earth & Planetary Science Letters, v. 196, p. 17-33.
Stein, C.A., and Stein, S., 1992, A model for the global variation in oceanic depth and heat flow with lithospheric age: Nature, v. 359, p. 123-129.
Stein, C.A., and Stein, S., 1994, Constraints on hydrothermal heat flux through the oceanic lithosphere from global heat flow: Journal of Geophysical Research, B, Solid Earth and Planets, v. 99, p. 3081-3095.
Steinberger, B., and Torsvik, T.H., 2008, Absolute plate motions and true polar wander in the absence of hotspot tracks: Nature, v. 452, p. 620-624.
Taylor, B., 2006, The single largest oceanic plateau: Ontong Java-Manihiki-Hikurangi: Earth and Planetary Science Letters, v. 241, p. 372-380.
Tripati, A., and Elderfield, H., 2005, Deep-sea temperature and circulation changes at the Paleocene-Eocene thermal maximum: Science, v. 308, p. 1894.
Van der Voo, R., Spakman, W., and Bijwaard, H., 1999, Mesozoic subducted slabs under Siberia: Nature, v. 397, p. 246-249.
Viso, R.F., Larson, R.L., and Pockalny, R.A., 2005, Tectonic evolution of the Pacific-Phoenix-Farallon triple junction in the South Pacific Ocean: Earth and Planetary Science Letters, v. 233, p. 179-194.